Published online 22 February 2018

Nucleic Acids Research, 2018, Vol. 46, No. 8 ***3981–3992***
doi: 10.1093/nar/gky114

Pathogenic CTC1 mutations cause global genome instabilities under replication stress

Yuan Wang and Weihang Chai*

Department of Biomedical Sciences, Elson S. Floyd College of Medicine, Washington State University, PO Box 1495, Spokane, WA 99210, USA

Received October 23, 2017; Revised February 01, 2018; Editorial Decision February 02, 2018; Accepted February 09, 2018

ABSTRACT

Coats plus syndrome is a complex genetic disorder that can be caused by mutations in genes encoding the CTC1–STN1–TEN1 (CST) complex, a conserved single-stranded DNA binding protein complex. Studies have demonstrated that mutations identified in Coats plus patients are defective in telomere maintenance, and concluded that Coats plus may be caused by telomere dysfunction. Recent studies have established that CST also plays an important role in countering replication stress and protecting the stability of genomic fragile sites. However, it is unclear whether instabilities at genomic regions may promote Coats plus development. Here, we characterize eleven reported disease-causing CTC1 missense and small deletion mutations in maintaining genome stability. Our results show that these mutations induce spontaneous chromosome breakage and severe chromosome fragmentation that are further elevated by replication stress, leading to global genome instabilities. These mutations abolish or reduce CST interaction with RAD51, disrupt RAD51 foci formation, and/or diminish binding to GC-rich genomic fragile sites under replication stress. Furthermore, CTC1 mutations limit cell proliferation under unstressed condition and significantly reduce clonal viability under replication stress. Results also suggest that the aa 600–989 region of CTC1 contains a RAD51-interacting domain. Our findings thus provide molecular evidence linking replication-associated genomic defects with CP disease pathology.

INTRODUCTION

Faithful DNA replication is critical to preventing detrimental replication errors and maintaining genome integrity. Genome replication frequently encounters numerous obstacles arising from endogenous and exogenous sources that slow or stall replication forks, disrupting proper progression of replication and threatening genome stability. To ensure genome integrity, cells have evolved a panoply of mechanisms to repair stalled replication. In response to fork stalling, multiple proteins regulating DNA damage response, DNA repair, replication and cell cycle checkpoints are activated to stabilize stalled forks and restart replication. Failure in restarting stalled replication results in fork collapse, contributing to DNA damage and genome instability. Not surprisingly, defects in resolving replication stress have been associated with the pathology of human genetic diseases linked to cancer, aging, neurological disorders, growth retardation and developmental defects (reviewed in (1)).

Coats plus (CP) is a genetic disease characterized by multi-system abnormalities of the eye, brain, bone, gastrointestinal system, and other parts of the body (2). Genetic studies have revealed that CP is primarily caused by dysfunction of the CTC1 and STN1 genes (3–7), which encode two subunits of the CST (CTC1–STN1–TEN1) complex, a trimeric protein complex that preferentially binds to G-rich single-stranded DNA including telomeric DNA (8–10). CP patients inherit CTC1 mutations in a compound heterozygous manner, with one allele encoding a frameshift or nonsense mutant and the other a missense mutant (3,5,6). Up to date, exome sequencing of CP patients has found nine frameshift, ten missense and two in-frame deletion mutations in the CTC1 gene (3,5,6,11). The frameshift mutants generate truncated protein and repressed expression levels of missense mutations of CTC1 (12).

CST is a major regulator of telomere maintenance. The yeast homolog of CST, Cdc13–Stn1–Ten1, plays a critical role in telomere capping and controls telomerase access to telomeres (13). Mammalian CST retains conserved functions in facilitating efficient replication of telomeric DNA, promoting C-strand synthesis, and restricting telomerase access to telomeres (9,14–17). CTC1-null mice display rapid telomere loss, accompanied by global proliferative defects and premature death due to bone marrow failure (18). CTC1 mutations and at least one STN1 mutation identified in CP patients display telomere dysfunction and severe reduction in proliferation, suggesting that the pathogenesis of CP may derive from cellular proliferation failure origi-

*To whom correspondence should be addressed. Tel: +1 509 358 7575; Fax: +1 509 358 7882; Email: wchai@wsu.edu

nating from telomere maintenance catastrophe (3,7,12,19). Interestingly, CP patients present clinical features distinct from other telomere dysfunction diseases such as dyskeratosis congenita (DC). In particular, retinal telangiectasia and exudates, intracranial calcification, and gastrointestinal bleeding observed in CP individuals are absent in DC cases. However, the molecular bases of CP remain incompletely understood.

Recent studies have demonstrated that CST also plays a key role in promoting genome-wide replication recovery after replication stress (10,15). CST deficiency induces the fragility of non-telomeric GC-rich repetitive sequences, contributing to spontaneous chromosome breakage and high-level chromosome fragmentation (10). One mechanism contributing to how CST promotes replication recovery is that CST may recruit RAD51, which is a key player in restoring stalled replication (20–23), to stalled sites in order to restart stalled replication (10). Yet, the precise mechanism underlying CST's role in replication recovery remains to be defined.

It remains unknown whether CST's function in replication recovery plays a role in disease development. Given the important function of CST in genome-wide replication recovery, we postulate that CP may be associated with genomic replication defect. In this study, we determine the effects of disease-causing CTC1 mutations on global genome stability and characterize the molecular defects. Our results show that CTC1 mutations induce spontaneous chromosome instabilities including breaks, gaps, fragmentations that are further elevated by replication stress. These mutations either disrupt RAD51 foci formation, attenuate or abolish CST interaction with RAD51, and reduce CTC1 binding to genomic fragile sequences under replication stress. Our results extend CP mutations to genomic replication defects, and indicate that the molecular deficiency in modulating RAD51 function may contribute to disease development.

MATERIALS AND METHODS

Plamids and stable shRNA knockdown

WT and mutant pCL-Myc-CTC1 plasmids, and pCI-neo-Myc-STN1, pcDNA-HA-TEN1 plasmids were described previously (8,10,19). All pCL-Myc-CTC1 constructs were converted to RNAi-resistant by QuikChange II XL Site-Directed Mutagenesis Kit (Agilent), and then sequenced to ensure sequence accuracy. CTC1 shRNA sequence targeted GAAAGTCTTGTCCGGTATT (shCTC1), and control siRNA targeted luciferase and the sequence was CGUACGCGGAAUACUUCGA (shLUC) (10). HeLa stably expressing RNAi-resistant Myc-CTC1 were generated by retroviral transduction followed by puromycin selection. Selected cells were then infected with retroviruses expressing shCTC1, followed by hygromycin to obtain cells with depletion of endogenous CTC1.

Cell culture

293T and HeLa cells were cultured in DMEM supplemented with 10% calf serum at 37°C containing 5% CO_2.

Antibodies

The following primary antibodies were used: rabbit polyclonal anti-CTC1 (Abcam), mouse monoclonal anti-Myc (Santa Cruz), mouse monoclonal anti-Myc (Millipore), mouse monoclonal anti-Flag (Sigma), rabbit polyclonal anti-RAD51 (Santa Cruz), rabbit polyclonal anti-RAD51 (Abcam), mouse monoclonal anti-HA (Sigma), mouse monoclonal anti-β-Actin (Sigma). Secondary antibodies were horseradish peroxidase-conjugated anti-mouse IgG (BD Biosciences) and anti-rabbit IgG (Vector Laboratories) for western blotting, DyLight 488-anti-mouse IgG (ThermoFisher) and DyLight 550-anti-rabbit IgG (ThermoFisher) for immunofluorescence.

MTT assay

Cells were seeded into 96-well multiplates at a density of 1 × 10^4 per well. Following overnight incubation, cells were treated with HU at indicated concentrations for 48 h. Subsequently, 20 μl 5 mg/ml MTT ([3-(4,5-dimethylthiazol-2-y)-2,5-diphenyltetrazolium bromide, 5 mg/ml)] were added to each well and incubated at 37°C for additional 4 h. Medium was then removed and 150 μl DMSO was added to dissolve the resulting formazan crystals. Light absorption was measured at 490 nm with a microplate spectrophotometer (BioTek Instrucments, Inc., Winooski, VT, USA). Graphs shown are representative of three independent experiments, each performed in triplicate.

Clonogenic survival assay

One hundred cells were seeded in 6-well dishes in triplicates one day prior to exposure to HU (0.8 mM, 24 h). Following treatment, media were removed and fresh media without HU were added. After 10 days in regular media, colonies were fixed with 6% glutaraldehyde and stained with 0.5% crystal violet for counting.

Chromosome breakage/fragmentation/shattering assay

Chromosome fragmentation assay was performed as described (10). For detecting chromosome breakage, metaphase images were acquired with MetaSystem® microscope with a 63× objective. For detecting chromosome fragmentation and shattering, images were acquired with Zeiss AxioImager M2 epifluorescence microscope 100× objective.

Co-immunoprecipitation (co-IP)

Cells were lysed in lysis buffer (0.1% NP-40, 50 mM Tris–HCl, pH 7.4, 50 mM NaCl, 2 mM DTT) supplemented with protease inhibitor cocktail (Roche), sonicated and centrifuged at 13 000 rpm for 15 min at 4°C. Supernatants were immunoprecipated with anti-RAD51 antibody or anti-HA affinity beads overnight at 4°C with constant rotation. Beads were then washed with cold lysis buffer at 4°C for three times, then resuspended in lysis buffer with SDS sample loading buffer, boiled for 5 min, and subject to western blot analysis. Three independent co-IP experiments were performed for each mutant to ensure reproducibility.

Immunofluorescence (IF) staining

Cells grown on cover slips or chamber slides were fixed with 4% paraformaldehyde for 15 min and then permeabilized with 0.15% Triton X-100 for 15 min. After washing with PBS three times, fixed cells were blocked with 5% BSA at 37°C for 1 h in humidified chamber, then incubated with primary antibodies for overnight at 4°C. Samples were then washed with PBS three times, and then incubated with secondary antibodies at room temperature for 1 h. Nuclei were visualized by DNA staining with DAPI mounting medium (Vector Laboratories). Z-stack images were obtained at a 0.3 μm thickness per slice under Zeiss AxioImager M2 epifluorescence microscope 100× objective. Single Z-slice images were selected as a representative image.

Chromatin immunoprecipitation (ChIP)

ChIP was carried out as previously described (10). Briefly, HeLa cells stably expressing WT or mutant Myc-CTC1 were treated with 2 mM HU for 20 h, and crosslinked with 1% formaldehyde. Crosslinked cells were resuspended in lysis buffer (50 mM Tris–HCl pH 8.0, 10 mM EDTA, pH 8.0, 1% Triton X-100, 1% SDS, 1 mM PMSF) supplemented with protease inhibitor cocktail (Roche) and sonicated three times at 10 s each. After centrifugation at 13 000 rpm for 15 min, supernatant was precleared with protein G beads (Roche) at 4°C for 1 h, and precleared lysate was then incubated with 5 μg of anti-Myc antibody at 4°C overnight. Subsequently, antibodies were captured by incubation with protein G beads at 4°C for 3 h. After centrifugation at 3000 rpm for 2 min, beads were washed by buffer A (0.1% SDS, 1% Triton X-100, 2 mM EDTA, 20 mM Tris–HCl, pH8.0, 150 mM NaCl, 1 mM PMSF) once, buffer B (0.1% SDS, 1% Triton X-100, 2 mM EDTA, 20 mM Tris–HCl, pH 8.0, 500 mM NaCl) once, buffer C (250 mM LiCl, 1% NP-40, 1% Na-Deoxycholate, 1 mM EDTA, 10 mM Tris–HCl pH 8.0) once, and buffer D (1 mM EDTA, 10 mM Tris–HCl pH 8.0) twice. Beads-bound proteins were eluted with elution buffer (1% SDS, 100 mM $NaHCO_3$) twice at 55°C for 15 min each, followed by incubation with 200 mM NaCl and proteinase K at 65°C overnight to reverse crosslinking. Eluted DNA was then ethanol precipitated and resuspended in TE buffer.

Quantitative PCR (qPCR)

ChIP DNA was analyzed by qPCR with StepOnePlus (Life Technologies) using SYBR Green Master Mix (Life Technologies). Primers for qPCR were described previously (10). In ChIP-PCR quantification, the standard comparative cycle threshold method ($\Delta\Delta C_T$ method) (24) was used to measure the amount of DNA. The amount of ChIP DNA was then normalized to input DNA amount, followed by subtraction of ChIP DNA amount from IgG control samples (25). qPCR assays were performed in duplicates from three independent ChIP experiments. Detailed qPCR conditions are described in Supplementary Information.

RESULTS

CTC1 mutations exhibit spontaneous chromosomal instabilities that are further elevated by replication stress

We have found that CST deficiency induces severe genome instability, causing spontaneous chromosome breakage and high-level fragmentation of mitotic chromosomes that can be further elevated by replication stress (10). To determine whether CP mutations were defective in maintaining genome stability, we generated a total of eleven RNAi-resistant CTC1 missense and small deletion mutations that were reported in CP patients (Figure 1A), stably expressed them in HeLa cells using retroviral transduction, and then depleted endogenous CTC1 with shRNA (Figure 1B). Metaphase cells were then collected from either untreated or hydroxyurea (HU)-treated samples and subject to chromosome fragmentation assay. Chromosomes appeared as morphologically intact condensed structure in control cells (shLUC). Without replication stress, CTC1 depletion increased the level of spontaneous chromosome breaks and gaps (Figure 1D), indicating that CTC1 is important for maintaining genome stability. HU exposure elevated chromosome abnormalities in CTC1 depleted cells, and generated high-level chromosome fragmentation and extensive shattering (Figure 1C and E). While RNAi-resistant wild-type (WT) CTC1 fully rescued chromosome abnormalities induced by CTC1 knockdown, all eleven mutations failed to completely rescue (Figure 1D and E). Among them, C-terminal mutants (L1142H and 1196-Δ7) were most deleterious and null, while N-terminal mutants like A227V and V259M displayed partial restoration of CTC1 function (Figure 1D and E). Our results suggest that CTC1 mutations are defective in maintaining global genome stability, and replication stress exacerbates such defects.

CTC1 mutations impair RAD51 foci formation in response to replication stress

RAD51 is a key player in rescuing stalled replication. Upon fork stalling, RAD51 is recruited to stalled sites to stabilize stalled forks and participates in multiple pathways to restart stalled replication (20–23). We have demonstrated that replication stress-induced RAD51 foci is significantly reduced by suppression of CTC1, STN1 or TEN1. In addition, CST deficiency diminishes RAD51 recruitment to fragile sequences, leading to the postulation that CST may facilitate RAD51 recruitment to stalled sites to promote replication restart (10). We hypothesized that disease-causing mutations might impair RAD51 function at stalled forks. To test this, we assessed the effects of CTC1 mutations on RAD51 foci formation under replication stress (Figure 2). Consistent with our previous findings (10), replication stress-induced RAD51 foci was abolished by CTC1 depletion (Figure 2 and Supplementary Figure S2). Expression of RNAi-resistant WT CTC1 restored RAD51 foci formation in knockdown cells (Figure 2 and Supplementary Figure S2). Among the eleven mutants, V665G, R840W, R975G, C985Δ, L1142H and 1196-Δ7 significantly reduced the percentage of RAD51 foci positive (RAD51+) cells (Figure 2B). In addition, the mean RAD51 fluorescence signal strength was diminished to the same level as that in CTC1-

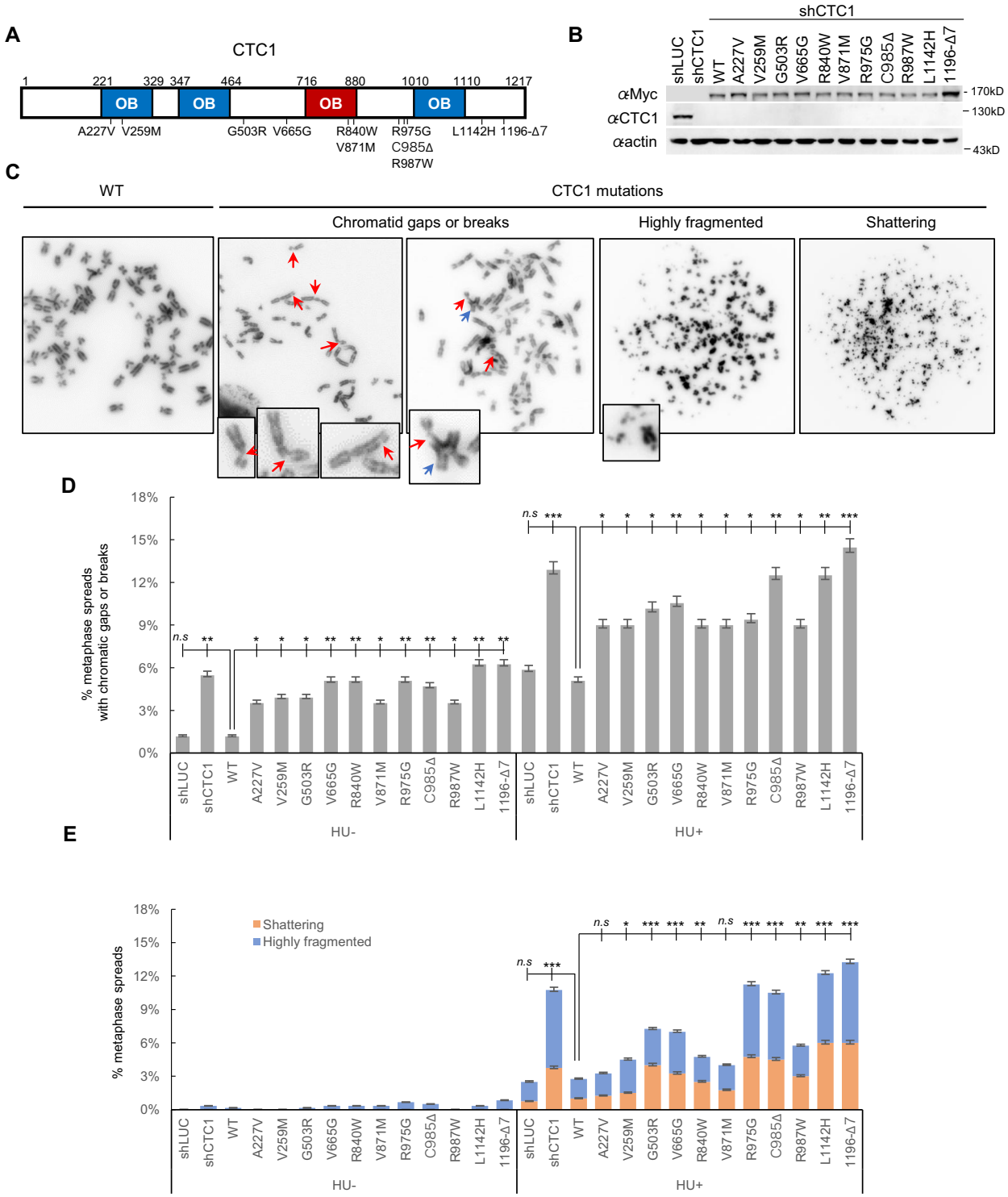

Figure 1. CTC1 mutations increases spontaneous chromosome breakage and induce high-level chromosome fragmentation and shattering under replication stress. (**A**) Schematic structure of human CTC1, with indication of mutations reported in CP patients. Blue and red boxes indicate the predicted and reported OB-folds, respectively. (**B**) Western blot showing the expression of exogenous Myc-CTC1 and knockdown of endogenous CTC1 in HeLa cells stably co-expressing shCTC1 and RNAi-resistant Myc-CTC1. Anti-CTC1 antibody detected endogenous CTC1 and enriched Myc-CTC1 (Supplementary Figure S1). (**C**) Representative metaphase images showing chromosomal abnormalities including breaks and gaps (indicated by red arrows), radial chromosomes (blue arrow), highly fragmented chromosomes, and chromosome shattering in cells expressing WT or mutant Myc-CTC1 with endogenous CTC1 being depleted. Detailed abnormalities are shown in amplified inserts. (**D**) Percentage of metaphase spreads with chromosome breaks/gaps with or without HU treatment. Results were from two independent experiments. >250 metaphase spreads were measured in each sample. Binomial Z statistic pairwise comparison was used for statistical analysis. Error bars, SEM. $*P \leq 0.05$, $**P \leq 0.01$, $***P \leq 0.001$. (**E**) Percentage of metaphase spreads with chromosome fragmentation/shattering with or without HU treatment. Results were from two independent experiments. >400 metaphase spreads were measured in each sample. Chi-squared test was used for statistical analysis. Error bars, SEM. $*P \leq 0.05$, $**P \leq 0.01$, $***P \leq 0.001$.

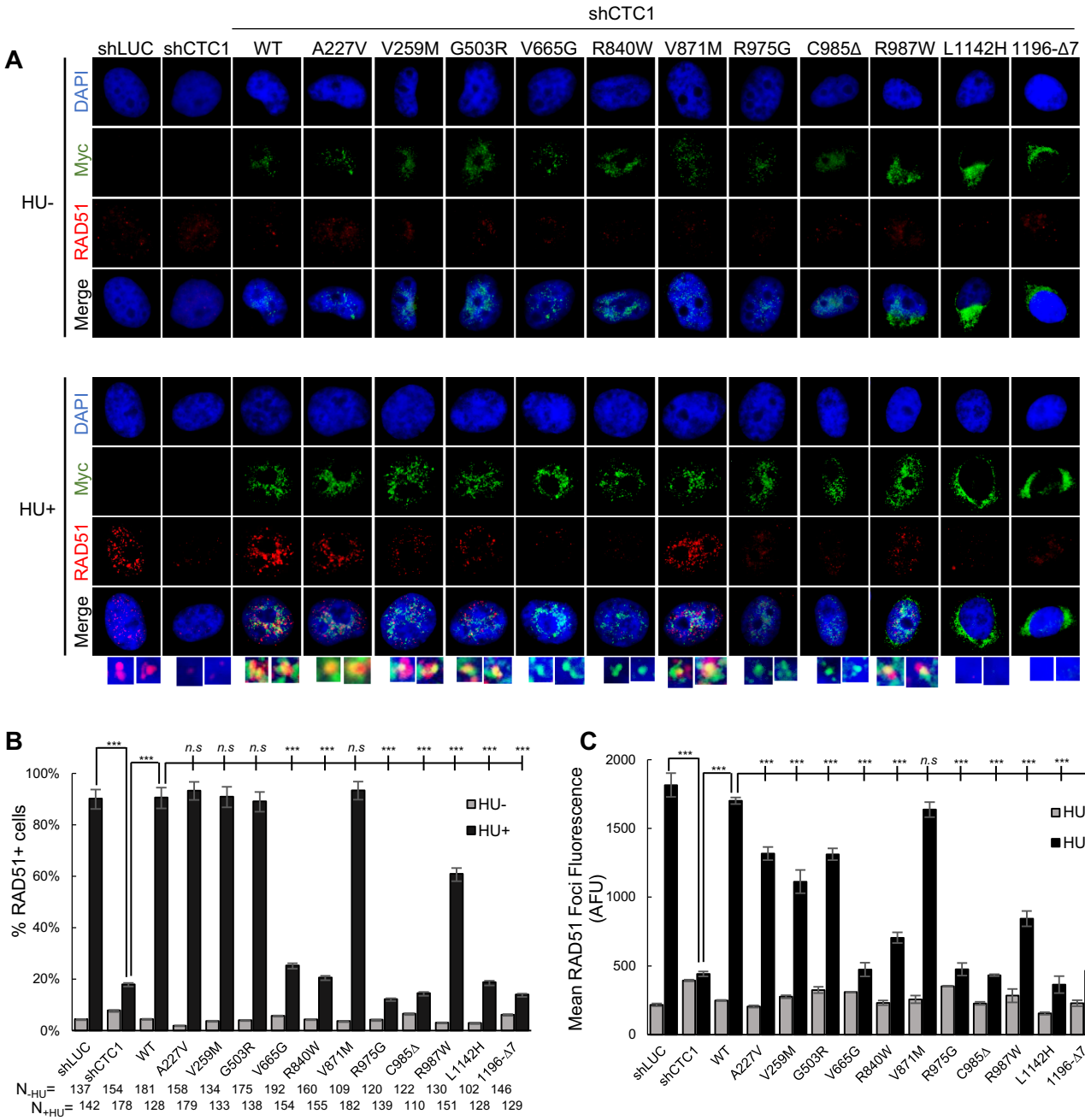

Figure 2. CTC1 mutations impair RAD51 foci formation after replication stress (see also Supplementary Figure S2). (**A**) IF of RAD51 (red) and Myc-CTC1 (green) in HeLa cells expressing RNAi-resistant WT or mutant Myc-CTC1 as indicated. Endogenous CTC1 was depleted with shCTC1 in all Myc-CTC1 expressing cells. Cells were treated with or without HU (2 mM) for 20 hrs prior to IF. The enlarged view of RAD51/Myc-CTC1 colocalization (yellow) is shown in inserts. Enlarged full images are provided in Supplemental Figure S2. (**B**) Proportion of cells containing ≥5 RAD51 foci. *N* denotes the number of cells measured in each sample. Binomial z statistic pairwise comparison was used for statistical analysis. Error bars, SEM. (**C**) Mean fluorescence of RAD51 per cell after HU treatment. One-way ANOVA analysis was used for statistical analysis. Error bars, SEM. $*P \leq 0.05$, $**P \leq 0.01$, $***P \leq 0.001$.

depleted cells (Figure 2C), indicating that these mutants failed to rescue RAD51 foci formation. Meanwhile, the R987W mutation displayed an intermediate rescue, showing a partial restoration of RAD51+ cells and RAD51 fluorescence (Figure 2B and C). Other mutations, including A227V, V259M and G503R, were able to induce RAD51 foci formation but showed attenuated mean RAD51 fluorescence signal strength, indicating that these mutants partially restored RAD51 recruitment in response to replication stress (Figure 2B and C).

Only a subset of Myc-CTC1 foci colocalized with RAD51, consistent with our previous results that replication stress-induced CST foci partially colocalize with RAD51 (10), and supporting that CST may be implicated in several pathways of genome maintenance via both RAD51-dependent and -independent pathways.

The majority of CTC1 mutations were predominantly enriched in the nucleus, while L1142H, 1196-Δ7 and a portion of R987W accumulated in cytoplasm (Figure 2A and Supplementary Figure S2). Our results partially agree with the previous study, which describes cytoplasmic localization of these three mutants (19). The same study also reported that two additional mutations A227V and V259M localize in cytoplasm (19), while a separate study shows that A227V and V259M localize more in nucleus than in cytosol (12). It is possible that such discretion may be due to differences in cell lines used in two studies. Regardless, it is likely that L1142H and 1196-Δ7 results in different compartmentalization with nuclear STN1/TEN1 and nuclear RAD51, which abolishes the assembly of nuclear CST complex as well as the failure to recruit RAD51.

The remaining mutations formed distinct nuclear foci after HU treatment. Colocalization with RAD51 foci was detected in A227V, V259M, G503R, V871M and R987W (Figure 2A), in agreement with the observation that these mutations were partially functional in RAD51 foci formation (Figure 2B and C).

Effect of CTC1 mutations on CST/RAD51 interaction

It appears that the formation of the trimeric CST complex is important for its biological function, as the high binding affinity to DNA is only achieved when the trimeric complex is formed (8,26). Supporting this, mutations disrupting CST complex formation localize in cytoplasm ((19) and Figure 2A in this study) and are deficient in binding to telomeres (19). In our co-IP assays, RAD51 either pulled down all three components of CST simultaneously, or failed to pull down any of them (Figure 3A), suggesting that CST likely interacted with RAD51 as a complex. Thus, we assessed whether the loss of CST/RAD51 interaction was due to the disruption of CST complex formation by CTC1 mutants. Myc-STN1, HA-TEN1 and WT or mutant Myc-CTC1 were co-expressed in 293T cells, and then CST was precipitated from extracts with anti-HA antibody (Figure 3B). We found that L1142H and 1196-Δ7 disrupted CTC1 binding to TEN1 and significantly weakened STN1-TEN1 interaction (Figure 3B), in agreement with the previous report (19). Our results suggest that the CST complex formation is required for interacting with RAD51. Meanwhile, V665G, R975G and C985Δ all retained CST complex formation (Figure 3B), indicating that the CST complex formation alone is insufficient for CST/RAD51 interaction, and other molecular functions of CST are likely involved in promoting CST/RAD51 interaction.

The aa 600–989 region of CTC1 participates in CST/RAD51 interaction

It is possible that amino acids V665, R975 and C985 may be structurally positioned at a region involved in RAD51/CST interaction. To determine this, we constructed a series of N-terminal truncations (Supplementary Figure S3). Since the CST complex formation is required for CST/RAD51 interaction (Figure 3) and the C-terminus of CTC1 is the binding domain for STN1/TEN1 (Figure 3 and (19)), the C-terminus was kept. Truncated mutations ΔN600 and ΔN840 removed regions upstream of V665, and R975/C985, respectively, and ΔN990 retained the C-terminal 227 residues (Supplementary Figure S3A). WT or each mutant was coexpressed with Myc-STN1 and HA-TEN1 in 293T cells, and co-IP was used to assess CST/RAD51 interaction in response to replication stress. Results showed that both ΔN600 and ΔN840 co-IPed with STN1/TEN1 (Supplementary Figure S3, top blot). While ΔN600 retained RAD51 interaction, ΔN840 partially reduced RAD51 interaction (Supplementary Figure S3, middle blot). CTC1ΔN990 not only disrupted CST complex formation (Supplementary Figure S3, top blot) but also resulted in instability of STN1 and TEN1 (Supplementary Figure S3, bottom blot). Not surprisingly, this mutant failed to interact with RAD51 (Supplementary Figure S3, middle blot). Together, our results suggest that aa 600–989 may contain a RAD51-interacting domain, within which R975 and C985 may reside in the region being particularly crucial for RAD51 binding, and V665 likely facilitates such interaction.

CTC1 mutations reduce association to fragile sequences after exposure to replication stress

CST associates with GC-rich repetitive non-telomeric fragile sites genome-wide after exposure to HU and protects the stability of these sequences under replication stress (10). We suspected that CTC1 mutants that abolished RAD51 interaction and RAD51 foci formation might also be defective in association with fragile sequences in the genome. We then used ChIP to determine CTC1 mutations association with four representative fragile sequences identified from our previous ChIP-seq analysis (HU4, HU8, HU10, HU12) (10). The majority of mutations significantly reduced association to these sequences, while A227V and R987W which showed moderately attenuated CTC1 association to selected fragile sites, (Figure 4). In agreement with STN1 binding observed in our previous study (10), CTC1 showed negligible binding to non-fragile sequences such as TUBLIN and SLITRK6 loci (Supplementary Figure S4). Thus, our results support that CP mutations compromise CTC1 association to genomic fragile sites in response to replication stress.

CTC1 mutations reduce cellular proliferation under unstressed condition and compromise clonal survival under replication stress

Given the spontaneous chromosome instabilities observed in CTC1 deficient cells (Figure 1), we tested whether CTC1 depletion affected cell proliferation. MTT assay showed that CTC1 depletion reduced cellular proliferation under normal culture condition (Figure 5A). Expressing RNAi-resistant WT-CTC1 fully rescued the proliferation defect (Figure 5A). An independent clonogenic assay confirmed that CTC1 depletion caused a reduction of clonal survival under unstressed condition (Figure 5B and C, HU- samples). Together, our results suggest that CTC1 is needed for optimal cellular growth and proliferation.

To test whether CTC1 mutations are more sensitive to replication stress, we performed clonogenic survival assay in HU. Clonal survival in CTC1 depleted cells was further

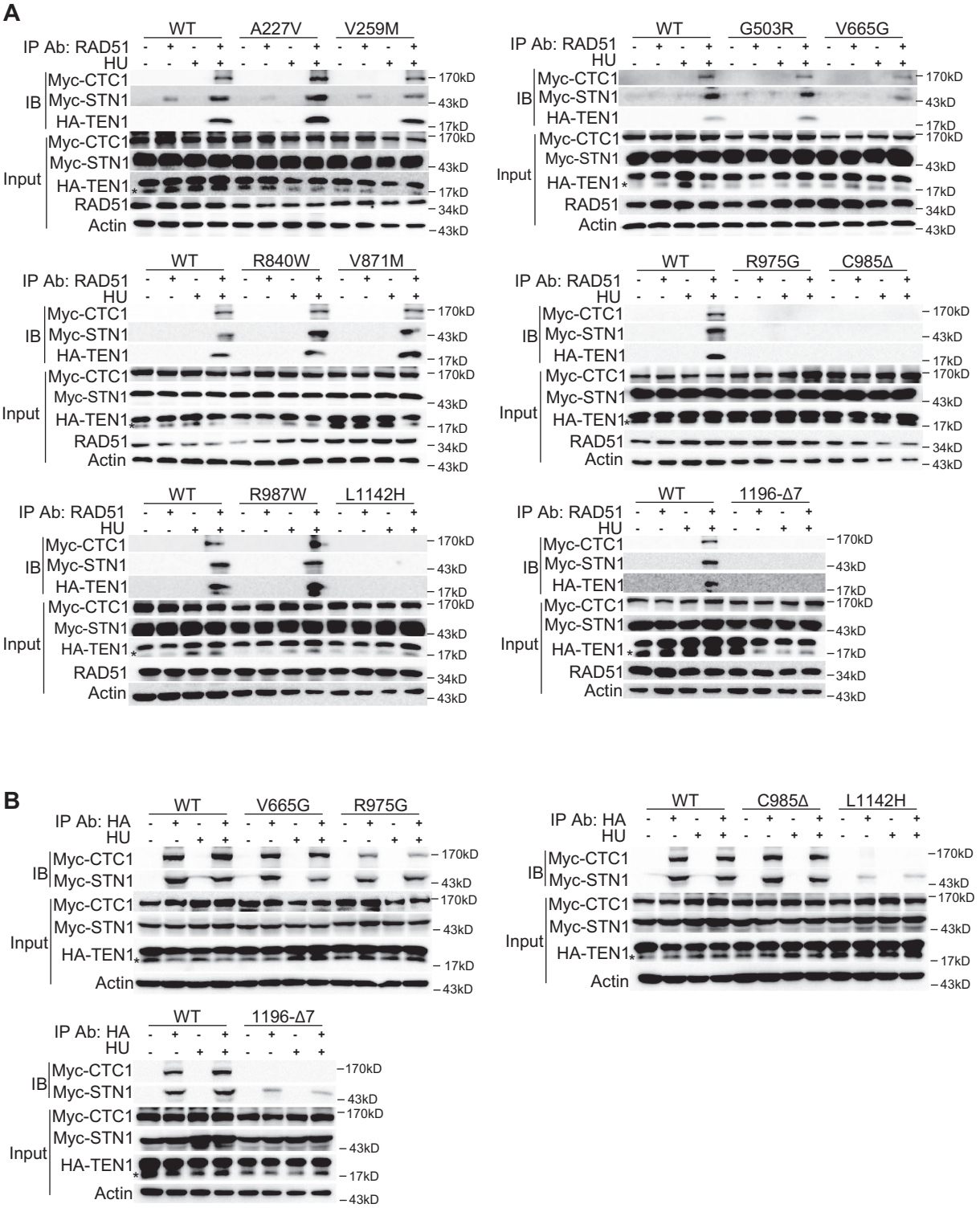

Figure 3. CTC1 mutations cause defects in molecular interaction with RAD51. (**A**) Interaction of CTC1 mutants with RAD51. Myc-STN1, HA-TEN1, WT or mutant Myc-CTC1 were transiently co-expressed in 293T cells, and cells were treated with or without HU (2 mM) for 20 h prior to co-IP with anti-RAD51 antibody. Precipitates were analyzed with western blotting to detect Myc-CTC1, Myc-STN1 and HA-TEN1 that were pulled down by RAD51. '*' indicates the non-specific band recognized by the HA antibody. (**B**) The ability of mutant CTC1 in CST complex formation. Myc-STN1, HA-TEN1, WT or mutant Myc-CTC1 were transiently co-expressed in 293T cells, and cells were treated with or without HU (2 mM) for 20 h prior to co-IP with anti-HA antibody, followed by western blotting to detect Myc-CTC1 and Myc-STN1 in the complex.

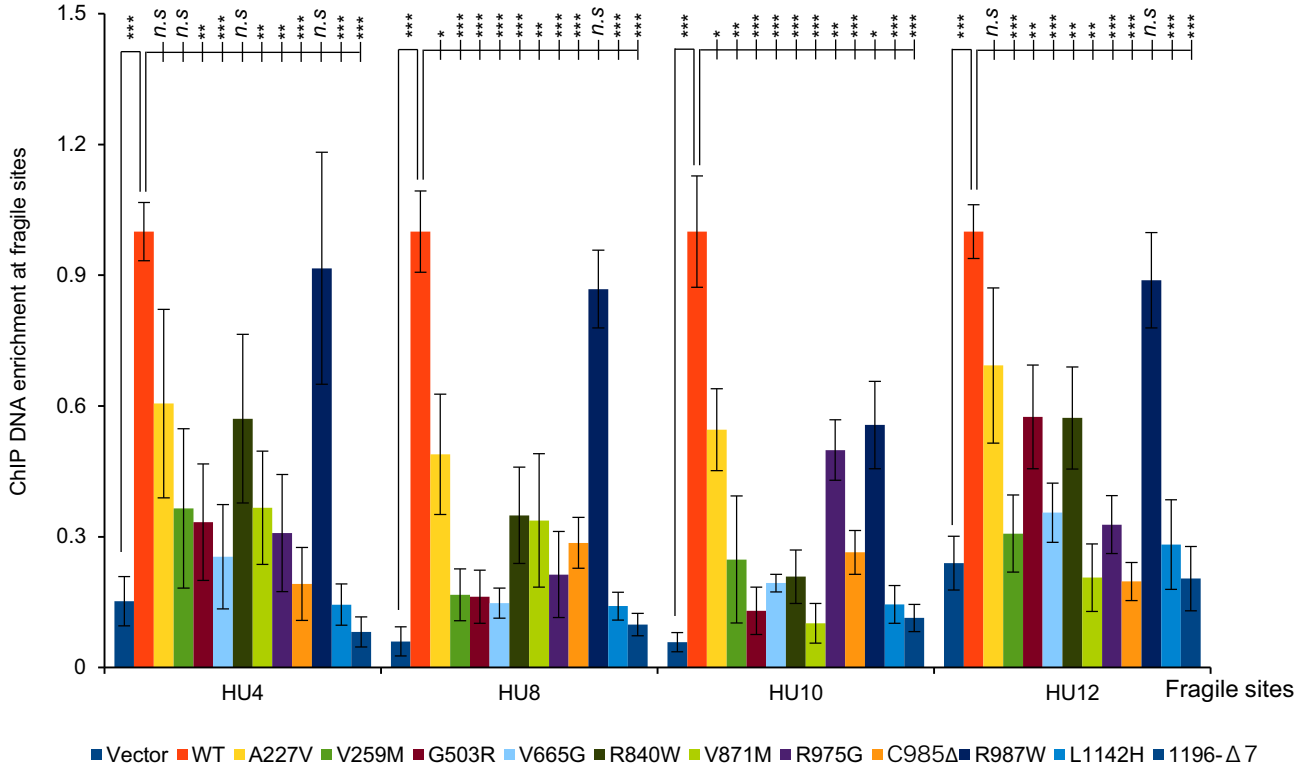

Figure 4. CTC1 mutations decrease binding to fragile sequences. HeLa cells stably expressing WT or mutant Myc-CTC1 were treated with HU, crosslinked, and ChIP-qPCR were performed. Three independent ChIP assays were carried out, with qPCR assays being performed in duplicates for each sample in each ChIP experiment. Results are represented as percentage of input and normalized to WT Myc-CTC1. Error bars, SEM. Kruskal Wallis with post hoc pairwise Wilxocan signed-rank test was used for statistical analysis. $*P \leq 0.05$, $**P \leq 0.01$, $***P \leq 0.001$. ChIP-qPCR results with non-fragile sequences are included in Supplemental Figure S4.

reduced after HU treatment (Figure 5C). Again, none of the disease-causing mutations was able to completely restore clonal viability (Figure 5C), indicating that these mutations are defective in promoting cell survival under replication stress.

DISCUSSION

CP is a complex developmental disorder with multi-system manifestations. Prior studies have shown that CST mutations identified in CP patients induce telomere maintenance defects (18,19). This is not surprising because CST is an important regulator of telomere homeostasis. It is also established that CST plays an important role in rescuing stalled replication genome-wide (10,15). Proteins involved in the recovery of stalled replication are important for efficient replication during processes that require increased cell proliferation, and have been directly implicated in the pathology of human diseases, many of which sharing similar phenotypic characteristics including developmental defects, growth retardation, and neurological disorders (1). Notably, CP patients display neurological disorders and vascular retinal defects distinct from other telomeropathy syndromes. In particular, retinal telangiectasia and exudates, intracranial calcification, and gastrointestinal bleeding observed in CP patients are not obvious in other telomeropathy cases (3,7). We therefore postulate that, in addition to telomere defects, non-telomeric replication defects caused by CST mutations and the resulting genome instabilities may play an important role in promoting CP pathogenesis. In this study, we show that eleven reported missense and small-deletion pathogenic CTC1 mutations fail to maintain chromosome stability and induce spontaneous chromosome breaks/gaps/fragmentations that can be elevated by replications stress. We also find that these mutations abolish or diminish CST binding to non-telomeric fragile sequences, disrupt CST/RAD51 interaction, and/or abrogate or reduce RAD51 foci formation in response to replication stress (Table 1). Lastly, clonal survival assays show that all disease-causing CTC1 mutations compromise clonal survival, and significantly reduce cellular viability under replication stress. Findings presented here support that, in addition to telomere defects, global genome damage resulting from impaired genome replication may also account for the development of CP in individuals carrying CST mutations.

Our analysis of genomic defects of CTC1 mutations suggests that these mutations may be divided into four groups (Table 1). The first group, represented by C-terminal mutations L1142H and 1196-Δ7, predominantly localize in cytosol, fail to form the CST complex, abolish DNA binding, and disrupt interaction with nuclear RAD51. They display loss-of-function in suppressing genome-wide replication stress, indicating they are null mutants. The null phenotype is likely owing to non-nuclear localization of these

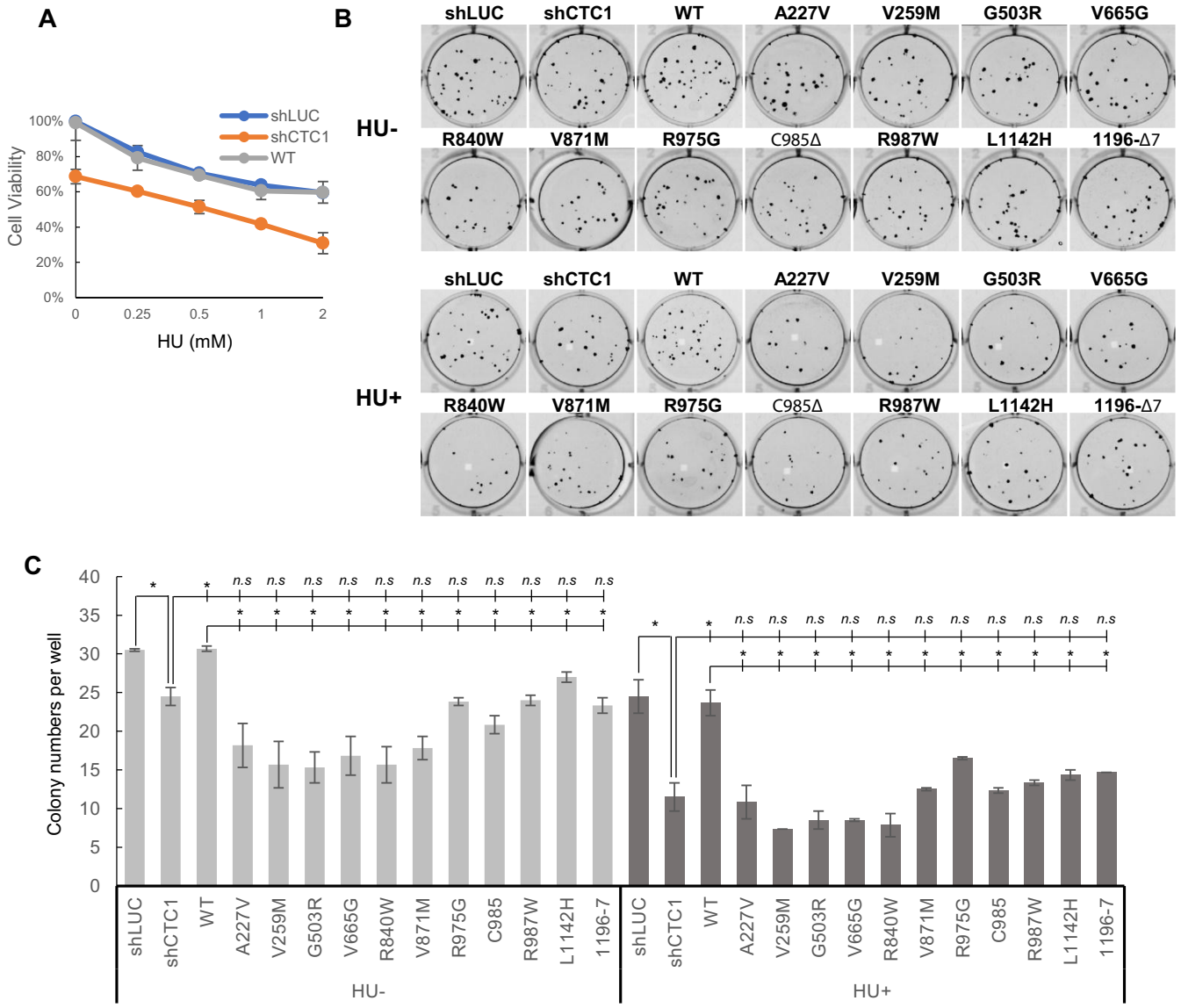

Figure 5. CTC1 mutations diminishes cellular proliferation and clonal survival. (**A**) MTT assay from HeLa cells expressing shLUC, shCTC1, or co-expressing shCTC1 and RNAi-resistant WT-CTC1. (**B**) Clonal survival of HeLa cells expressing CTC1 mutations with and without HU treatment. Except for shLUC control, all cells were depleted of endogenous CTC1. Results from two independent experiments were plotted in (**C**). Two-tailed *t*-test was used for calculating *P* values. Error bars, SEM. $*P \leq 0.05$, $**P \leq 0.01$, $***P \leq 0.001$.

Table 1. Summary of molecular defects caused by CTC1 mutations under replication stress

	WT	A227V	V259M	G503R	V665G	R840W	V871M	R975G	C985Δ	R987W	L1142H	1196-Δ7
Spontaneous chr breaks/gaps	-	+	+	+	++	++	+	++	++	+	++	++
HU-induced breakage	-	+	+	+	++	+	+	+	++	+	++	+++
HU-induced chr fragmentation	-	-	+	+++	+++	++	-	+++	+++	++	+++	+++
Proliferation	◆▶	▼	▼	▼	▼	▼	▼	▼	▼	▼	▼	▼
HU sensitivity	-	+	+	+	+	+	+	+	+	+	+	+
RAD51 interaction	+	+	+	+	±	+	+	-	-	+	-	-
RAD51 foci formation	+	±	±	±	-	-	+	-	-	±	-	-
Fragile sites association	+	±	±	-	-	±	-	-	-	±	-	-
Localization	N	N	N	N	N	N	N	N	N	N + C	C	C

two mutants and their inability to form the CST complex, which are essential for CST function. Consistently, no patients carried homozygous alleles of these two, in combination with each other, or in combination with frame-shift alleles with presumed complete loss-of-function, indicating such combination would be lethal.

The second group includes C985Δ, R975G, R840W, V665G and G503R. They retain CST complex formation while induce chromosome instabilities and HU sensitivity. This group abolishes or attenuates RAD51 foci formation, presumably due to their inability to bind to fragile sites and/or interact with RAD51, which may impair RAD51 recruitment to stalled replication sites. They are thus predicted to result in disease manifestation.

While this manuscript was in revision, an OB-fold domain spanning aa 716–880 was reported (27). This OB-fold resides within the aa 600 to 989 region that is critical for RAD51 interaction (Supplementary Figure S3), indicating that this OB-fold may contribute to CST/RAD51 interaction (Figure 6).

Mutations A227V, V259M and R987W consist of the third group with partial genomic phenotypes. They partially rescue chromosome breakage/gaps/fragmentation induced by CTC1 depletion (Figure 1D, E), suggesting that their impacts on full-length CTC1 is limited. Consistently, they compromise DNA binding only at selected fragile sites (Figure 4), present moderate effects on RAD51 foci formation (Figure 2), and have no obvious impact on RAD51 interaction (Figure 3). The partial genomic defects conferred by these three mutants are reminiscent to their partial telomeric phenotypes. Their counterpart mutations in mammalian CTC1 display mild increase in telomere loss and telomere fusion (12). C-strand fill-in appears to be unaffected by A227V, R840W, R987W (12). In addition, A227V and R987W show no statistical significant increase of ExoI-resistant ss telomere DNA, indicating that telomere replication is largely not impacted (19). It is conceivable that the added partial defects at both telomeric and non-telomeric regions may contribute to their overall survival deficiency.

The last group is V871M, which is unique from all other mutations in that it behaves like wildtype in all the characterized molecular functions, including CST complex formation ((12,19) and this study), RAD51 interaction, RAD51 foci formation (this study), POLα interaction, telomere association, and in vitro DNA binding (12,19). Surprisingly, it induces an increase in chromosomal instabilities (Figure 1D) and telomere dysfunction (12,19). V871M is located at the very C-terminus of the newly reported OB-fold (27). Though this OB domain is not involved in direct DNA binding in vitro, ChIP shows that it contributes to telomere binding in cells (27), consistent with our observation that V871M compromises binding to fragile sites (Figure 4). Thus, the ability to directly bind to ss DNA may not support sufficient chromatin association. Given that V871M contributes to the stability of the OB fold (27), it is possible that V871M may impair the overall stability and/or correct folding of full-length CTC1.

No reported CP patient carried two null alleles, indicating that complete loss of CTC1 would be embryonic lethal. All CP patients carry heterozygous compound mutations, with one point mutant *CTC1* allele combined with a frameshift or a truncated allele with presumed complete loss-of-function, or combined with another point mutant allele (Supplementary Table S1). Though the compound heterozygosity makes it difficult to correlate the clinical impacts with the observed molecular phenotypes, it seems that the severity of molecular defects aligns well with reported disease onset time (Supplementary Table S1). In general, patients carrying missense alleles with partial and weaker molecular defects (A227V, V259M, V871M, R987W in groups 3 and 4) show later onset of disease than those carrying mutant alleles showing more severe molecular defects in groups 1 and 2 (Supplementary Table S1).

Our analysis of disease-causing mutations, together with results from other groups (12,19), support that the assembly of the CST complex is crucial for CST function, and nuclear localization of CST relies on complex formation. Disrupting complex formation therefore results in a complete loss of function. Other molecular properties, including the ability to associate with telomeric and non-telomeric fragile sequences in cells, RAD51 interaction, and RAD51 recruitment are also important for the full function of CST. Partial loss of fragile sequence association, RAD51 recruitment, or RAD51 interaction lead to partial replication and telomere defects. Interestingly, direct in vitro binding to ss-DNA per se is not sufficient for chromatin association (19). Lastly, it is important to note that replication stress-induced CST foci partially colocalize with RAD51 (this study and (10)). It is conceivable that CST may promote genome stability via both RAD51-dependent and -independent pathways. One possible pathway may be related to the established function of CST in stimulating DNA POLα activity. CST was originally identified as an accessory factor of POLα and stimulates POLα priming activity and primase-to-polymerase switching (28–31). Up to now only three proteins have been found to interact with CST: RAD51, POLα, and TPP1. More CST binding partners are expected to be identified, which will aid in understanding the function of CST in replication stress response.

A recent study identifies a mutation in another telomere factor POT1 in CP cases (32). Analyses of fibroblasts derived from POT1 patients and one CTC1 patient (carrying heterozygous K242Lfs*41|G503R) show that they share similar telomere defects including elongated G-overhangs and truncated telomeres (32). Since POT1 is presumed to function specifically at telomeres, it is argued that CP is a telomere disease caused by defective C-strand fill-in (32). However, other studies report that certain CTC1 CP mutations do not significantly elongate G-overhangs (18,19), raising the possibility that subtypes of CP may exist. We postulate that in certain individuals, proliferation failure caused by severe telomere defects may be the primary drive for disease formation, while in other patients both replication and telomere defects play important roles in promoting CP development. Precisely how much telomere defects and how much replication defects contribute to CP development remain to be determined.

In conclusion, our findings from characterizing the effects of disease-causing mutations on replication restart provide molecular insights into the disease biology, which may offer guidance to the development of more effective therapeutic interventions for CP patients.

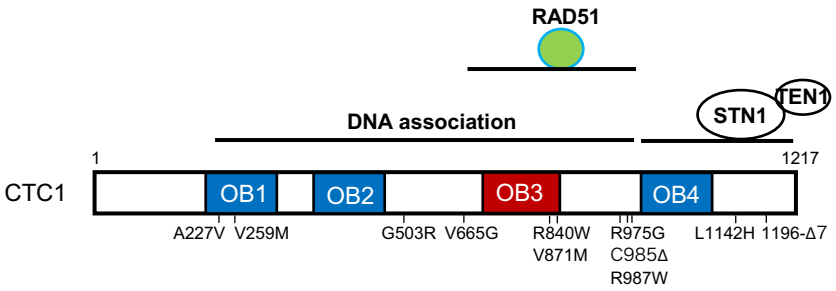

Figure 6. Depicted molecular domains of CTC1. Approximate depiction is derived from results from this study and previous reports (8,12,19,27). The C-terminus of CTC1, including OB4, is needed for complexing with STN1/TEN1. The aa 600–989 region includes the newly identified OB3 and may participate in RAD51 binding. DNA binding likely involves OB1, OB2 and residues between OB3 and OB4, though structural studies are needed to pinpoint the precise DNA-binding domains.

SUPPLEMENTARY DATA

Supplementary Data are available at NAR Online.

ACKNOWLEDGEMENTS

We thank Liuh-Yow Chen (Academia Sinica, Taiwan) for pCL-Myc-CTC1 constructs, and Robert Tsai (Texas A&M) for FLAG-RAD51 construct. We are grateful to Xinxing Lyu, Megan Chastain, Olga Shiva for technical help and helpful discussions.
Author contributions: Y.W. performed the majority of experiments and collected all the data. W.C. conceived and directed the study. Y.W. and W.C. wrote the paper.

FUNDING

National Institutes of Health [R01GM112864 to W.C.]. Funding for open access charge: National Institutes of Health [R01GM112864].
Conflict of interest statement. None declared.

REFERENCES

1. Zeman,M.K. and Cimprich,K.A. (2013) Causes and consequences of replication stress. *Nat. Cell Biol.*, **16**, 2–9.
2. Armanios,M. (2012) An emerging role for the conserved telomere component 1 (CTC1) in human genetic disease. *Pediatr. Blood Cancer*, **59**, 209–210.
3. Anderson,B.H., Kasher,P.R., Mayer,J., Szynkiewicz,M., Jenkinson,E.M., Bhaskar,S.S., Urquhart,J.E., Daly,S.B., Dickerson,J.E., O'Sullivan,J. *et al.* (2012) Mutations in CTC1, encoding conserved telomere maintenance component 1, cause Coats plus. *Nat. Genet.*, **44**, 338–342.
4. Keller,R.B., Gagne,K.E., Usmani,G.N., Asdourian,G.K., Williams,D.A., Hofmann,I. and Agarwal,S. (2012) CTC1 Mutations in a patient with dyskeratosis congenita. *Pediatr. Blood Cancer*, **59**, 311–314.
5. Polvi,A., Linnankivi,T., Kivela,T., Herva,R., Keating,J.P., Makitie,O., Pareyson,D., Vainionpaa,L., Lahtinen,J., Hovatta,I. *et al.* (2012) Mutations in CTC1, encoding the CTS telomere maintenance complex component 1, cause cerebroretinal microangiopathy with calcifications and cysts. *Am. J. Hum. Genet.*, **90**, 540–549.
6. Walne,A.J., Bhagat,T., Kirwan,M., Gitiaux,C., Desguerre,I., Leonard,N., Nogales,E., Vulliamy,T. and Dokal,I.S. (2013) Mutations in the telomere capping complex in bone marrow failure and related syndromes. *Haematologica*, **98**, 334–338.
7. Simon,A.J., Lev,A., Zhang,Y., Weiss,B., Rylova,A., Eyal,E., Kol,N., Barel,O., Cesarkas,K., Soudack,M. *et al.* (2016) Mutations in STN1 cause Coats plus syndrome and are associated with genomic and telomere defects. *J. Exp. Med.*, **213**, 1429–1440.
8. Miyake,Y., Nakamura,M., Nabetani,A., Shimamura,S., Tamura,M., Yonehara,S., Saito,M. and Ishikawa,F. (2009) RPA-like mammalian Ctc1-Stn1-Ten1 complex binds to single-stranded DNA and protects telomeres independently of the Pot1 pathway. *Mol. Cell*, **36**, 193–206.
9. Chen,L.Y., Redon,S. and Lingner,J. (2012) The human CST complex is a terminator of telomerase activity. *Nature*, **488**, 540–544.
10. Chastain,M., Zhou,Q., Shiva,O., Whitmore,L., Jia,P., Dai,X., Huang,C., Fadri-Moskwik,M., Ye,P. and Chai,W. (2016) Human CST facilitates genome-wide RAD51 recruitment to GC-rich repetitive sequences in response to replication stress. *Cell Rep.*, **16**, 1300–1314.
11. Lin,H., Gong,L., Zhan,S., Wang,Y. and Liu,A. (2017) Novel biallelic missense mutations in CTC1 gene identified in a Chinese family with Coats plus syndrome. *J. Neurol. Sci.*, **382**, 142–145.
12. Gu,P. and Chang,S. (2013) Functional characterization of human CTC1 mutations reveals novel mechanisms responsible for the pathogenesis of the telomere disease Coats plus. *Aging Cell.*, **12**, 1100–1109.
13. Giraud-Panis,M.J., Teixeira,M.T., Geli,V. and Gilson,E. (2010) CST meets shelterin to keep telomeres in check. *Mol. Cell*, **39**, 665–676.
14. Huang,C., Dai,X. and Chai,W. (2012) Human Stn1 protects telomere integrity by promoting efficient lagging-strand synthesis at telomeres and mediating C-strand fill-in. *Cell Res.*, **22**, 1681–1695.
15. Stewart,J.A., Wang,F., Chaiken,M.F., Kasbek,C., Chastain,P.D. 2nd, Wright,W.E. and Price,C.M. (2012) Human CST promotes telomere duplex replication and general replication restart after fork stalling. *EMBO J.*, **31**, 3537–3549.
16. Wang,F., Stewart,J. and Price,C.M. (2014) Human CST abundance determines recovery from diverse forms of DNA damage and replication stress. *Cell Cycle*, **13**, 3488–3498.
17. Kasbek,C., Wang,F. and Price,C.M. (2013) Human TEN1 maintains telomere integrity and functions in genome-wide replication restart. *J. Biol. Chem.*, **288**, 30139–30150.
18. Gu,P., Min,J.N., Wang,Y., Huang,C., Peng,T., Chai,W. and Chang,S. (2012) CTC1 deletion results in defective telomere replication, leading to catastrophic telomere loss and stem cell exhaustion. *EMBO J.*, **31**, 2309–2321.
19. Chen,L.Y., Majerska,J. and Lingner,J. (2013) Molecular basis of telomere syndrome caused by CTC1 mutations. *Genes Dev.*, **27**, 2099–2108.
20. Arlt,M.F., Durkin,S.G., Ragland,R.L. and Glover,T.W. (2006) Common fragile sites as targets for chromosome rearrangements. *DNA Repair (Amst.)*, **5**, 1126–1135.
21. Petermann,E. and Helleday,T. (2010) Pathways of mammalian replication fork restart. *Nat. Rev. Mol. Cell Biol.*, **11**, 683–687.
22. Petermann,E., Orta,M.L., Issaeva,N., Schultz,N. and Helleday,T. (2010) Hydroxyurea-stalled replication forks become progressively inactivated and require two different RAD51-mediated pathways for restart and repair. *Mol. Cell*, **37**, 492–502.
23. Hashimoto,Y., Chaudhuri,A.R., Lopes,M. and Costanzo,V. (2010) Rad51 protects nascent DNA from Mre11-dependent degradation and promotes continuous DNA synthesis. *Nat. Struct. Mol. Biol.*, **17**, 1305–1311.
24. Schmittgen,T.D. and Livak,K.J. (2008) Analyzing real-time PCR data by the comparative C(T) method. *Nat. Protoc.*, **3**, 1101–1108.

25. Haring,M., Offermann,S., Danker,T., Horst,I., Peterhansel,C. and Stam,M. (2007) Chromatin immunoprecipitation: optimization, quantitative analysis and data normalization. *Plant Methods*, **3**, 11.
26. Bryan,C., Rice,C., Harkisheimer,M., Schultz,D.C. and Skordalakes,E. (2013) Structure of the human telomeric Stn1-Ten1 capping complex. *PLoS One*, **8**, e66756.
27. Shastrula,P.K., Rice,C.T., Wang,Z., Lieberman,P.M. and Skordalakes,E. (2017) Structural and functional analysis of an OB-fold in human Ctc1 implicated in telomere maintenance and bone marrow syndromes. *Nucleic Acids Res.*, **46**, 972–984.
28. Casteel,D.E., Zhuang,S., Zeng,Y., Perrino,F.W., Boss,G.R., Goulian,M. and Pilz,R.B. (2009) A DNA polymerase-{alpha}{middle dot}primase cofactor with homology to replication protein A-32 regulates DNA replication in mammalian cells. *J. Biol. Chem.*, **284**, 5807–5818.
29. Nakaoka,H., Nishiyama,A., Saito,M. and Ishikawa,F. (2011) Xenopus laevis Ctc1-Stn1-Ten1 (xCST) complex is involved in priming DNA synthesis on single-stranded DNA template in Xenopus egg extract. *J. Biol. Chem.*, **287**, 619–627.
30. Lue,N.F., Chan,J., Wright,W.E. and Hurwitz,J. (2014) The CDC13-STN1-TEN1 complex stimulates Pol alpha activity by promoting RNA priming and primase-to-polymerase switch. *Nat. Commun.*, **5**, 5762.
31. Ganduri,S. and Lue,N.F. (2017) STN1-POLA2 interaction provides a basis for primase-pol alpha stimulation by human STN1. *Nucleic Acids Res.*, **45**, 9455–9466.
32. Takai,H., Jenkinson,E., Kabir,S., Babul-Hirji,R., Najm-Tehrani,N., Chitayat,D.A., Crow,Y.J. and de Lange,T. (2016) A POT1 mutation implicates defective telomere end fill-in and telomere truncations in Coats plus. *Genes Dev.*, **30**, 812–826.